

On the Numerical Solution of Some Semilinear Elliptic Problems – II

K. Atkinson, Iowa City and A. Sommariva, Padua

Received March 16, 2004; revised July 22, 2004

Published online: December 20, 2004

© Springer-Verlag 2004

Abstract

In the earlier paper [6], a Galerkin method was proposed and analyzed for the numerical solution of a Dirichlet problem for a semi-linear elliptic boundary value problem of the form $-\Delta U = F(\cdot, U)$. This was converted to a problem on a standard domain and then converted to an equivalent integral equation. Galerkin's method was used to solve the integral equation, with the eigenfunctions of the Laplacian operator on the standard domain D as the basis functions. In this paper we consider the implementing of this scheme, and we illustrate it for some standard domains D .

AMS Subject Classifications: 65R20, 65N99, 35J65.

Keywords: Elliptic, nonlinear, integral equation, Galerkin method.

1. Introduction

In the earlier paper [6], a Galerkin method is proposed and analyzed for the numerical solution of a Dirichlet problem for a semi-linear elliptic boundary value problem of the form

$$\begin{aligned} -\Delta U &= F(\cdot, U) && \text{on } \Omega, \\ U &= G && \text{on } \partial\Omega, \end{aligned} \tag{1}$$

where $\Omega \subset \mathbb{R}^2$ is a simply-connected open domain with a boundary $\partial\Omega$. We assume that there is a known conformal mapping from a standard open domain D to Ω , and we then reduce the problem (1) to an equivalent problem on D ,

$$\begin{aligned} -\Delta u &= f(\cdot, u) && \text{on } D, \\ u &= g && \text{on } \partial D. \end{aligned} \tag{2}$$

This equation is converted to an equivalent integral equation. We use Galerkin's method to solve the integral equation, with the eigenfunctions of the Laplacian operator on the standard domain D as the basis functions. In this paper, we consider the implementing of this scheme, and we illustrate it for some standard domains D .

In Sect. 2, we give some of the background from [6] that is needed here. We consider only the case of homogeneous boundary conditions, $u = 0$ on ∂D . The more general non-homogeneous condition can be treated by means of solving the Dirichlet problem for Laplace's equation,

$$\begin{aligned} -\Delta v &= 0 & \text{on } D, \\ v &= g & \text{on } \partial D, \end{aligned}$$

perhaps by means of a boundary integral equation. The solution v can then be used to modify the original problem (2) to one in which the boundary condition is simply zero; cf. [6]. In Sect. 3, we present theoretical results on the rate of convergence of the Galerkin method based on the eigenvalues of the associated potential theory problem on D . In Sects. 4, 5 and 6, we discuss and illustrate numerically the specific cases of D the unit square, the unit disk, and the upper half of the unit disk, respectively.

2. Galerkin's Method

Let $G(x, y; \xi, \eta)$ be the Green's function for the problem

$$\begin{aligned} -\Delta u &= \psi & \text{in } D, \\ u &= 0 & \text{on } \partial D \end{aligned}$$

assuming that ψ is known. Then the solution u to (2) satisfies

$$u(x, y) = \int_D G(x, y; \xi, \eta) f(\xi, \eta, u(\xi, \eta)) d\xi d\eta, \quad (x, y) \in \bar{D}. \quad (3)$$

As in [13], we introduce $v(x, y) = f(x, y, u(x, y))$. The function v is a solution of

$$v(x, y) = f\left(x, y, \int_D G(x, y; \xi, \eta) v(\xi, \eta) d\xi d\eta\right), \quad (x, y) \in \bar{D}. \quad (4)$$

Note also the discussion in [9]. After finding $v(x, y)$, we can calculate

$$u(x, y) = \int_D G(x, y; \xi, \eta) v(\xi, \eta) d\xi d\eta, \quad (x, y) \in \bar{D}.$$

A formula for the actual calculation of our approximations to $u(x, y)$ is given below in (10).

We use Galerkin's method to solve (4). To do this, we consider the eigenvalue problem for the Laplacian operator:

$$\begin{aligned} -\Delta \phi &= \lambda \phi & \text{in } D, \\ \phi &= 0 & \text{on } \partial D. \end{aligned} \quad (5)$$

Let $0 < \lambda_1 \leq \lambda_2 \leq \dots \rightarrow \infty$ be the sequence of the eigenvalues, and ϕ_1, ϕ_2, \dots be corresponding eigenfunctions. The existence of the eigenpair sequence is guaranteed, and the eigenfunctions can be chosen to form an orthogonal basis of $L^2(D)$; cf. [14]. Then we have

$$\begin{aligned} -\Delta\phi_j &= \lambda_j\phi_j & \text{in } D, \\ \phi_j &= 0 & \text{on } \partial D, \end{aligned} \quad (6)$$

or,

$$\int_D G(x, y; \xi, \eta) \phi_j(\xi, \eta) d\xi d\eta = \frac{1}{\lambda_j} \phi_j(x, y), \quad (x, y) \in \bar{D}, \quad j = 1, 2, \dots \quad (7)$$

Let

$$\mathcal{X}_n = \text{span}\{\phi_1, \dots, \phi_n\}.$$

The Galerkin method for (4) is to find

$$v_n = \sum_{j=1}^n \alpha_j \phi_j \in \mathcal{X}_n$$

such that

$$(v_n, \phi_i) = \left(f(x, y, \int_D G(x, y; \xi, \eta) v_n(\xi, \eta) d\xi d\eta), \phi_i \right), \quad 1 \leq i \leq n, \quad (8)$$

i.e., upon using the orthogonality of $\{\phi_i\}_i$,

$$\alpha_i (\phi_i, \phi_i) = \int_D \phi_i(x, y) f\left(x, y, \sum_{j=1}^n \frac{\alpha_j}{\lambda_j} \phi_j(x, y)\right) dx dy, \quad 1 \leq i \leq n. \quad (9)$$

The advantage of applying the Galerkin method to solve the auxiliary problem (4) is that the integral

$$\int_D G(x, y; \xi, \eta) v_n(\xi, \eta) d\xi d\eta = \sum_{j=1}^n \frac{\alpha_j}{\lambda_j} \phi_j(x, y)$$

is available and has been computed exactly. If we apply the Galerkin method directly to the problem (3), in each iteration for solving the resulting nonlinear algebraic system we would have to evaluate double integrals

$$\int_D \int_D G(x, y; \xi, \eta) f(\xi, \eta, u_n^{(k)}(\xi, \eta)) \phi_i(x, y) d\xi d\eta dx dy, \quad 1 \leq i \leq n,$$

where, the superscript (k) is the iteration index. Another advantage of the method is that the left side of the system (9) is diagonal; this may bring in some convenience in solving (9) numerically.

After we compute the Galerkin solution $v_n = \sum_{j=1}^n \alpha_j^{(*)} \phi_j$, we can generate an approximation of u using

$$\begin{aligned} u_n(x, y) &= \int_D G(x, y; \zeta, \eta) v_n(\zeta, \eta) d\zeta d\eta \\ &= \sum_{j=1}^n \frac{\alpha_j^{(*)}}{\lambda_j} \phi_j(x, y), \quad (x, y) \in \bar{D}. \end{aligned} \tag{10}$$

2.1. Convergence Analysis

Introduce the Nemyckii operator

$$(\mathcal{F}(u))(x, y) = f(x, y, u(x, y)), \tag{11}$$

and the linear integral operator

$$(\mathcal{G}(v))(x, y) = \int_D G(x, y; \zeta, \eta) v(\zeta, \eta) d\zeta d\eta. \tag{12}$$

Equations (3) and (4) are written symbolically as

$$u = \mathcal{G}\mathcal{F}(u), \tag{13}$$

$$v = \mathcal{F}(u),$$

$$v = \mathcal{F}(\mathcal{G}v). \tag{14}$$

Let \mathcal{P}_n be the $L^2(D)$ orthogonal projection of $L^2(D)$ onto \mathcal{X}_n , where the eigenfunctions ϕ_j have unit norm. Then the Galerkin solution $v_n \in \mathcal{X}_n$ of (8) satisfies the operator equation

$$v_n = \mathcal{P}_n \mathcal{F}(\mathcal{G}v_n). \tag{15}$$

Also, (10) is written symbolically by

$$u_n = \mathcal{G}v_n. \tag{16}$$

Natural assumptions on \mathcal{F} and \mathcal{G} are given in [6], together with an error analysis. In particular, denote an isolated solution (13) by u^* and let $v^* = \mathcal{F}(u^*)$. Then for n sufficiently large, say $n \geq N$, the approximating Eq. (15) has a solution v_n that is unique in some neighborhood of v^* that is independent of n . Moreover,

$$\|v^* - v_n\| \leq (1 + \delta_n) \|v^* - \mathcal{P}_n v^*\|, \quad n \geq N \tag{17}$$

with $\delta_n \rightarrow 0$. Also,

$$\|u^* - u_n\|^2 \leq \frac{1}{\lambda_1^2} \delta_n (2 + \delta_n) \|v^* - \mathcal{P}_n v^*\|^2 + \|u^* - \mathcal{P}_n u^*\|^2. \quad (18)$$

The norm is that of $L^2(D)$. Additional error analysis results are given in [6].

3. Speed of Convergence

In order to discuss the speed of convergence, we need to bound the Fourier error $\|u^* - \mathcal{P}_n u^*\|$ for $u^* \in H_0^2(D)$. Again, assume that the eigenvalues satisfy

$$0 < \lambda_1 \leq \lambda_2 \leq \dots \leq \lambda_m \leq \dots$$

and also assume that the corresponding eigenfunctions $\{\phi_j\}$ are orthonormal. We give an error bound for $\|u^* - u_n\|$ based on the speed with which the eigenvalues increase in size. We begin with some preliminary extensions of the theory presented in the preceding Sect. 2.

Recall that

$$\begin{aligned} u^* &= \mathcal{G}v^*, \\ u_n &= \mathcal{G}v_n. \end{aligned}$$

Subtracting,

$$u^* - u_n = \mathcal{G}(v^* - v_n). \quad (19)$$

Applying \mathcal{P}_n to (14) and manipulating,

$$v^* = v^* - \mathcal{P}_n v^* + \mathcal{P}_n \mathcal{F}(\mathcal{G}v^*).$$

Subtracting (15),

$$v^* - v_n = v^* - \mathcal{P}_n v^* + \mathcal{P}_n \mathcal{F}(\mathcal{G}v^*) - \mathcal{P}_n \mathcal{F}(\mathcal{G}v_n).$$

Using (19),

$$u^* - u_n = \mathcal{G}(v^* - \mathcal{P}_n v^*) + \mathcal{G} \mathcal{P}_n [\mathcal{F}(u^*) - \mathcal{F}(u_n)].$$

As mappings on $L^2(D)$ it is easily checked that

$$\mathcal{P}_n \mathcal{G} = \mathcal{G} \mathcal{P}_n$$

and therefore,

$$u^* - u_n = u^* - \mathcal{P}_n u^* + \mathcal{P}_n \mathcal{G} [\mathcal{F}(u^*) - \mathcal{F}(u_n)]. \quad (20)$$

Using the Frechét differentiability of \mathcal{F} at u^* ,

$$\mathcal{F}(u^*) - \mathcal{F}(u_n) = \mathcal{F}'(u^*)(u^* - u_n) + O(\|u^* - u_n\|^2).$$

Substituting this into (20) and then rearranging terms,

$$[I - \mathcal{P}_n \mathcal{G} \mathcal{F}'(u^*)](u^* - u_n) = u^* - \mathcal{P}_n u^* + O(\|u^* - u_n\|^2). \tag{21}$$

The operator $\mathcal{G} \mathcal{F}'(u^*)$ is compact on $L^2(D)$ to $L^2(D)$. We assume that 1 is not an eigenvalue of $\mathcal{G} \mathcal{F}'(u^*)$; it follows, therefore, that

$$I - \mathcal{G} \mathcal{F}'(u^*) : L^2(D) \xrightarrow[\text{onto}]{1-1} L^2(D). \tag{22}$$

In [6, theorem 6] it is assumed that 1 is not an eigenvalue of the compact operator $\mathcal{F}'(u^*)\mathcal{G}$, and the rationale for this is discussed there. It is straightforward to show that 1 is not an eigenvalue of $\mathcal{F}'(u^*)\mathcal{G}$ if and only if 1 is not an eigenvalue of $\mathcal{G} \mathcal{F}'(u^*)$; and thus our assumption is equivalent to that already discussed in the cited reference.

Since \mathcal{P}_n converges pointwise to I on $L^2(D)$, it follows that

$$\|(I - \mathcal{P}_n)\mathcal{G} \mathcal{F}'(u^*)\| \rightarrow 0 \quad \text{as } n \rightarrow \infty.$$

Combining this with (22), and applying the geometric series theorem, we have that $[I - \mathcal{P}_n \mathcal{G} \mathcal{F}'(u^*)]^{-1}$ exists for all sufficiently large n , say $n \geq N$, and these inverses are uniformly bounded in n ,

$$\left\| [I - \mathcal{P}_n \mathcal{G} \mathcal{F}'(u^*)]^{-1} \right\| \leq B < \infty, \quad n \geq N.$$

Applying this to (21), we obtain

$$\|u^* - u_n\| \leq O(\|u^* - \mathcal{P}_n u^*\|). \tag{23}$$

A more detailed derivation of these results can be carried out in the manner of [7].

Since $u \in L^2(D)$,

$$\begin{aligned} u^*(P) &= \sum_{j=1}^{\infty} (u^*, \varphi_j) \varphi_j(P), \quad P \in D \\ \|u^*\|_{L^2} &= \sqrt{\sum_{j=1}^{\infty} |(u^*, \varphi_j)|^2} < \infty. \end{aligned} \tag{24}$$

Introduce

$$\begin{aligned} g &= -\Delta u^*, \\ u^* &= \mathcal{G}g. \end{aligned}$$

Then using the symmetry of the operator \mathcal{G} ,

$$\begin{aligned} \|u^*\|_{L^2} &= \sqrt{\sum_{j=1}^{\infty} |(u^*, \varphi_j)|^2} = \sqrt{\sum_{j=1}^{\infty} |(\mathcal{G}g, \varphi_j)|^2} = \sqrt{\sum_{j=1}^{\infty} |(g, \mathcal{G}\varphi_j)|^2} \\ &= \sqrt{\sum_{j=1}^{\infty} \frac{|(g, \varphi_j)|^2}{\lambda_j^2}}. \end{aligned} \tag{25}$$

Similarly,

$$\begin{aligned} u^*(P) - \mathcal{P}_n u^*(P) &= \sum_{j=n+1}^{\infty} (u^*, \varphi_j) \varphi_j(P), \\ \|u^* - \mathcal{P}_n u^*\| &= \sqrt{\sum_{j=n+1}^{\infty} |(u^*, \varphi_j)|^2} = \sqrt{\sum_{j=n+1}^{\infty} \frac{|(g, \varphi_j)|^2}{\lambda_j^2}} \\ &\leq \frac{1}{\lambda_{n+1}} \sqrt{\sum_{j=n+1}^{\infty} |(g, \varphi_j)|^2} = \frac{1}{\lambda_{n+1}} \|g - \mathcal{P}_n g\|. \end{aligned} \tag{26}$$

Combining with (23),

$$\|u^* - u_n\| = o(\lambda_{n+1}^{-1}) \quad \text{as } n \rightarrow \infty. \tag{27}$$

We can also analyze the speed of uniform convergence of $\mathcal{P}_n u^*$ to u^* , but for this we need additional information on the size of $\|\phi_j\|_{\infty}$. We omit such a discussion here.

Example 1: *When the domain is the square $D = (0, \pi) \times (0, \pi)$, the eigenvalues and associated orthonormal eigenfunctions are*

$$\lambda_{m,n} = m^2 + n^2, \quad u_{m,n}(x, y) = \frac{2}{\pi} \sin(mx) \sin(ny), \quad m, n = 1, 2, \dots \tag{28}$$

It makes sense to replace the subspaces \mathcal{X}_n with the following approximating subspaces:

$$\mathcal{X}_\ell = \{u_{m,n} \mid m^2 + n^2 < \ell\} \tag{29}$$

for $\ell = 1, 2, 3, \dots$. The dimension of \mathcal{X}_ℓ is of size $O(\ell)$. The bound (27) becomes

$$\|g - \mathcal{P}_\ell g\| \leq o(\ell^{-1}). \tag{30}$$

4. Calculations on the Square

We begin by discussing our computational framework for the numerical examples of this and the following sections. We must set up and then solve the nonlinear system (9). We solve the system using a version of Broyden’s iteration method. The setup and iteration requires numerical integration over the region D . In practice, a fixed tolerance TOL is provided by the user, and we want to find n for which

$$\|u_n - u^*\| \leq TOL \tag{31}$$

for some norm $\|\cdot\|$. We discuss later the approximation of $\|u_n - u^*\|$.

Let $m_k = 2^k$ and consider the first m_k distinct eigenvalues of $-\Delta$ (not repeated even when multiple),

$$\lambda_1 < \dots < \lambda_{m_k} \tag{32}$$

and an orthogonal basis $\{\phi_i \mid i = 1, \dots, n_k\}$ of the associated eigenfunctions, $n_k \geq m_k$. Using the iterative method to solve the nonlinear system (9), we begin with the case $n = n_1$. Denote the solution to this system by $\alpha_{n_1}^{(*)} = \{\alpha_{i,n_1}^{(*)}\}_{i=1}^{n_1}$. When a sufficiently good approximation $\tilde{\alpha}_{n_1} = \{\tilde{\alpha}_{i,n_1}\}_{i=1}^{n_1}$ of $\alpha_{n_1}^{(*)}$ is computed, we check whether

$$\tilde{E}_{n_1} := \left\| \sum_{j=1}^{n_1} \frac{\tilde{\alpha}_{j,n_1}}{\lambda_j} \phi_j - u^* \right\| \leq TOL. \tag{33}$$

(This, of course, requires some more accurate way of estimating u^* , a point we return to later.) If not, we use $\alpha_{n_2}^{(0)} = (\tilde{\alpha}_{n_1}, 0, \dots, 0) \in \mathbb{R}^{n_2}$ as a starting point for the system (9) in which $n = n_2$. When $\tilde{\alpha}_{n_2}$ is computed, check whether $\tilde{E}_{n_2} \leq TOL$. If yes, then computation is completed. Otherwise we begin another level and use the initial guess $\alpha_{n_3}^{(0)} = (\tilde{\alpha}_{n_2}, 0, \dots, 0) \in \mathbb{R}^{n_3}$, and we repeat the process until for a certain n_k , we have $\tilde{E}_{n_k} \leq TOL$.

We observe that in view of the convergence of the Fourier series for $v^* \in L^2(D)$, the coefficients of v^* tend to 0; and the same is therefore true for those of u^* , as is implied also by (25). This fact implies that at larger levels, the starting point is usually a rather good approximation of the solution $\alpha_{n_k}^{(*)}$ and in general few iterations of the iterative method are necessary to compute u_{n_k} . Moreover, for $k > 1$, the result provided by the nonlinear scheme at the first iteration at level k , say $\alpha_{n_k}^{(1)}$ is such that

$$\tilde{E}_{n_{k-1}} \approx \left\| \sum_{j=1}^{n_k} (\alpha_{j,n_k}^{(1)} - \alpha_{j,n_k}^{(0)}) \frac{\phi_j}{\lambda_j} \right\|.$$

Hence, a good *a posteriori* estimate of the error at the previous level is available.

We implemented our algorithm in *Matlab*, using Broyden’s method as the non-linear solver (see also [3], [11]). In particular, we adopted the “limited memory” routine *brsol* of [10]. We did not observe any particular benefit to using the more advanced procedures *brsola* (a clever implementation of the Broyden-Armijo algorithm) since the convergence of *brsol* was already quite fast.

Some observations are necessary:

- (1) Depending on the domain D , the integrals in (9) have been computed by a suitable quadrature rule, generally with some type of Gaussian quadrature with a high degree of precision.. On the square we used the *Matlab* program *dblquad*. On the disk we used a product rule based upon the trapezoidal rule for the angular variable and Gauss-Legendre quadrature for the radial variable; and on the upper half of the unit disk, we use a product rule based on Gauss-Legendre in both the angular and radial variables.
- (2) We modified the stopping criterion of *brsol*, since we are more interested in computing an approximation u_n of the solution u^* than we are in the coefficients $\alpha_n^{(*)}$. Consequently, instead of the weighted test on the residual originally present in the code, we use at the i -th iteration of the nonlinear scheme the test

$$\begin{aligned} \|u_n^{(i+1)} - u_n^{(i)}\|_{2,w} &:= \frac{1}{\sqrt{n}} \|u_n^{(i+1)} - u_n^{(i)}\|_2 \\ &= \frac{1}{\sqrt{n}} \left\| \left\{ \frac{(\alpha_{j,n}^{(i+1)} - \alpha_{j,n}^{(i)}) \|\phi_j\|_2}{\lambda_j} \right\}_{j=1}^n \right\|_2 \leq \varepsilon_{n_k}, \end{aligned}$$

where $\varepsilon_{n_{k+1}} = c\tilde{E}_{n_k}$ with $c = 10^{-3}$, i.e., the tolerance of Broyden method at level $k + 1$ is a fraction of the error \tilde{E}_{n_k} at the previous level.

- (3) For solving (9) we calculate the zeros of $F = \{F_i\}_{i=1}^n$, where

$$\begin{aligned} F_i(z) = & z_i - \frac{1}{(\phi_i, \phi_i)} \int_D \phi_i(x, y) \\ & \times f\left(x, y, \sum_{j=1}^n \frac{z_j}{\lambda_j} \phi_j(x, y)\right) \sim dx dy, \quad i = 1, \dots, n. \end{aligned} \tag{34}$$

In our numerical tests, this formulation results in far fewer iterations than when F is defined directly using (9). This is primarily of significance for the cases of the disk and semi-disk. Of course, if we had normalized all of the eigenfunctions ϕ_i to length 1, the formulations of F_i would have been the same; but the most convenient definitions of ϕ_i were not so normalized.

4.1. Numerical Example on Square

In the case of a rectangle $D = [0, a] \times [0, b]$ with $a, b > 0$, it is well known that the eigenvalues of $-\Delta$ are

$$\lambda_{m,n} = \pi^2 \left(\frac{m^2}{a^2} + \frac{n^2}{b^2} \right), \quad m, n = 1, 2, \dots \tag{35}$$

and the corresponding eigenfunctions are

$$u_{m,n}(x, y) = \sin\left(\frac{m\pi x}{a}\right) \sin\left(\frac{n\pi y}{b}\right), \quad m, n = 1, 2, \dots \tag{36}$$

To simplify the computations, and without any loss of generality, we work on the square $D = [0, \pi] \times [0, \pi]$. In our numerical experiments, as in [6], we choose as a basis for $L^2(D)$ the orthonormal set

$$u_{m,n}(x, y) = \frac{2}{\pi} \sin(mx) \sin(n\pi y), \quad m, n = 1, 2. \tag{37}$$

The only point to be discussed is the ordering of the eigenvalues $\{\lambda_j\}$ and the definition of the associated eigenfunctions $\{\phi_j\}$. Although there are several ways to order the eigenvalues $\lambda_{m,n} = m^2 + n^2$, we opted for the natural one based on their magnitude, as in (32). In passing we observe that if $\lambda_i = \lambda_{m,n}$ for some (m, n) , we also have $\lambda_i = \lambda_{n,m}$. This fact implies that, except for the case in which is $m = n$, any eigenvalue has (at least!) two distinct eigenfunctions.

As a numerical example for this paper, we consider the elliptic semilinear equation

$$\begin{cases} -\Delta u(x, y) = e^{-u(x,y)} + g(x, y), & (x, y) \in D \\ u(x, y) = 0, & (x, y) \in \partial D \end{cases} \tag{38}$$

where, for

$$\bar{u}(x, y) = x(\pi - x)y(\pi - y)e^{x \cos(y)}, \tag{39}$$

we have set $g(x, y) = -e^{-\bar{u}(x,y)} - \Delta u(x, y)$. The solution of (38) is \bar{u} . This solution was chosen to ensure there was no favorable numerical behavior due to symmetry in the solution u . Figure 1 shows the first 512 Fourier coefficients $c_j = (\bar{u}, \phi_j)$, $j \geq 1$, of \bar{u} ; most are nonzero and they are decreasing fairly slowly.

In the numerical experiments, we need to evaluate the approximate solution \tilde{u}_N on some grid in D . We have fixed in the square $[0, \pi] \times [0, \pi]$ the points $(x_j, y_k) = (\frac{j\pi}{10}, \frac{k\pi}{10})$, for $j, k = 0, \dots, 10$, and then computed

$$\begin{aligned} \tilde{E}_{2w}^{(N_\phi)} &:= \frac{1}{11} \sqrt{\sum_{j,k=0}^{10} [\tilde{u}_{N_\phi}(x_j, y_k) - \bar{u}(x_j, y_k)]^2}, \\ \tilde{E}_{G2w}^{(N_\phi)} &:= \frac{1}{11} \sqrt{\sum_{j,k=N_\phi}^{512} (\tilde{c}_j - \bar{c}_j)^2}. \end{aligned} \tag{40}$$

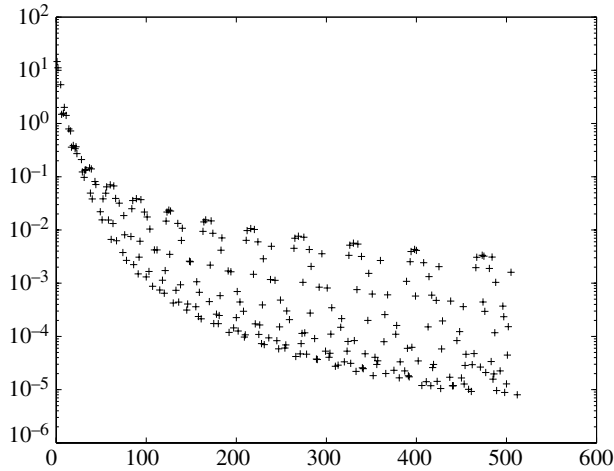


Fig. 1. Fourier coefficients for \bar{u} defined by (39)

Table 1. The Galerkin method applied to Eq. (38) on the square

N_λ	N_ϕ	\tilde{E}_{2w}	\tilde{E}_{G2w}	Ratio	Iterations
2	3	3.03E+0	9.68E+0	–	5
4	6	1.71E+0	5.47E+0	1.77	4
8	13	5.66E-1	1.81E+0	3.05	3
16	28	1.67E-1	5.63E-1	3.38	2
32	64	5.37E-2	1.73E-1	3.25	2
64	135	2.20E-2	7.21E-2	2.44	2

In this N_ϕ is the number of eigenfunctions, and \tilde{u}_{N_ϕ} is the solution to the boundary value problem relative to the problem of dimension N_ϕ . The quantity $\{\tilde{c}_j\}_{j=1}^{512}$ denotes the vector of the first N_ϕ Galerkin coefficients of \tilde{u}_{N_ϕ} computed by the method, followed by 0 components; and $\{\bar{c}_j\}_{j=1}^{512}$ are the first 512 Fourier coefficients of \bar{u} . Finally, *Ratio* denotes the quotient between two successive $\tilde{E}_{2w}^{(N_\phi)}$, and N_λ denotes the number of eigenvalues.

As seen in the table, the behaviour of the error in the method is almost linear in N_λ^{-1} . Figure 2 shows more clearly that there is a uniform behavior to the error; and it is linear with respect to N_ϕ^{-1} . There is numerical evidence that the solution \tilde{v}_{N_ϕ} of the integral equation in Kumar-Sloan form is a much rougher approximation of v than is \tilde{u}_{N_ϕ} when compared to \bar{u} . For example, with the notation already introduced, $\frac{1}{\Gamma} \sqrt{\sum_{j,k=0}^{10} [\tilde{v}_{64}(x_j, y_k) - \bar{v}(x_j, y_k)]^2} \approx 1.15 \times 10^1$ while $\tilde{E}_{2w}^{(64)} \approx 5.37 \times 10^{-2}$ from the above table ($N_\lambda = 32$).

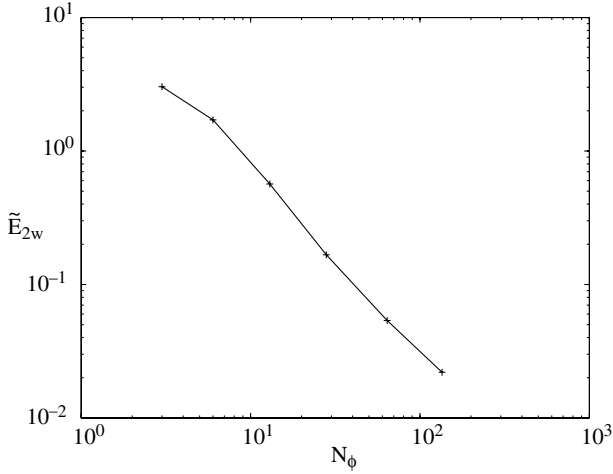


Fig. 2. Error over the square

5. Numerical Examples on the Unit Disk

In the case of the unit disk it is well known (cf. [14]) that if $j_{m,n}$ is the n -th positive zero of the Bessel function J_m , then the eigenvalues of $-\Delta$ are

$$\lambda_{m,n} = j_{m,n}^2, m = 0, 1, 2, \dots, n = 1, 2, \dots \tag{41}$$

and a set of corresponding orthogonal eigenfunctions are

$$\begin{cases} u_{0,n}(x, y) = J_0(j_{0,n}r), n = 1, 2, \dots \\ u_{m,n}^{(1)}(x, y) = J_m(j_{m,n}r) \cos(m\theta), m = 1, 2, \dots, n = 1, 2, \dots \\ u_{m,n}^{(2)}(x, y) = J_m(j_{m,n}r) \sin(m\theta), m = 1, 2, \dots, n = 1, 2, \dots \end{cases} \tag{42}$$

In particular,

$$\begin{cases} (u_{m,n}^{(1)}, u_{k,l}^{(2)}) = 0 \\ (u_{m,n}^{(1)}, u_{k,l}^{(1)}) = \frac{\pi}{2} [J'_m(j_{m,n})] \delta_{m,k} \delta_{n,l} \\ (u_{m,n}^{(2)}, u_{k,l}^{(2)}) = \frac{\pi}{2} [J'_m(j_{m,n})] \delta_{m,k} \delta_{n,l} \end{cases} \tag{43}$$

The vectors $\{u_{0,n}\}_{n=1}^\infty, \{u_{m,n}^{(1)}\}_{n=1}^\infty, \{u_{m,n}^{(2)}\}_{n=1}^\infty$ form an orthogonal basis of $L^2(D)$. Here, as usual, (\cdot, \cdot) is the scalar product in $L^2(D)$ and $\delta_{m,k}$ the Kronecker operator.

In the implementation, we need to order the $j_{m,n}$ in increasing order. To this end we have used *Mathematica* to list the zeros $j_{m,n}$ for $m = 0, 1, \dots, 70, n = 1, \dots, 20$, and we then sorted them within *Matlab*. Knowing some basic properties about the distribution of $j_{m,n}$, namely

$$j_{m,n} \sim \left(n + \frac{m}{2} - \frac{1}{4} \right) \pi \quad \text{as } n \rightarrow \infty.$$

We can guarantee that the first 512 numbers in the sorted list are exactly the first 512 positive Bessel zeros. At this point, by (41) and (42), it is straightforward to compute the eigenvalues and, using the *Matlab* routine *besselj*, the value of the eigenfunctions at any point (x, y) . Notice that the scalar products in (43) involve the derivative of Bessel functions. Since

$$xJ'_m(x) - mJ_m(x) = -xJ_{m+1}(x)$$

and $J_m(j_{m,n}) = 0$ we have $J'_m(j_{m,n}) = -J_{m+1}(j_{m,n})$, i.e. $J'_m(j_{m,n})$ can be directly computed using *besselj*.

Finally, to approximate numerically the integrals on the right-hand side of (8), we used the product formula by Stroud [15]

$$\int_D f(x, y) dx dy \approx I_N := h \sum_{j=0}^N \sum_{k=0}^{2N} w_k f(r_j e^{i\theta_k}), \tag{44}$$

where $h = \frac{2\pi}{2N+1}$ and $\{r_j\}, \{w_j\}$ are, respectively, the nodes and the weights of the Gauss-Legendre rule on $[0, 1]$. This formula has degree of precision $2N$ for polynomials $f(x, y)$. We increase the parameter N until $|I_N - I_{2N}|$ is less than or equal to $1/10$ of the Broyden method error tolerance.

As a particular example here, we consider the semi-linear elliptic Eq. (38) where $g = -\Delta \bar{u} - e^{-\bar{u}}$. We choose

$$\bar{u}(x, y) = (1 - x^2 - y^2)^q e^{x \cos(y)} \tag{45}$$

for this unit disk case. The solution of the problem is of course \bar{u} . Figure 3 shows the first 1004 Fourier coefficients $c_j = (\bar{u}, \phi_j)$, $j \geq 1$, of \bar{u} . The pattern is quite different than that for the square, with many of the coefficients being zero and the others converging to zero fairly rapidly. We tested the behavior of our code in the case of varying $q \geq 1$. Here we give results for only $q = 1$. We considered 2, 4, 8, 16, 32, 64, 128 eigenvalues; note that the number of eigenfunctions is approximately double this number.

We have fixed in the disk $B(0, 1)$ the points

$$(x_j, y_k) = \left(\frac{j}{10} \cos\left(\frac{2k\pi}{10}\right), \frac{j}{10} \sin\left(\frac{2k\pi}{10}\right) \right) \quad j, k = 0, \dots, 10$$

and then computed as in the case of the square the quantities $\tilde{E}_{2w}^{(N_\phi)}$, $\tilde{E}_{G2w}^{(N_\phi)}$ and *Ratio*: Figure 4 contains the graph of N_ϕ vs. \tilde{E}_{2w} , and it indicates that the error behavior is tending towards a linear dependence of \tilde{E}_{2w} on N_ϕ^{-1} .

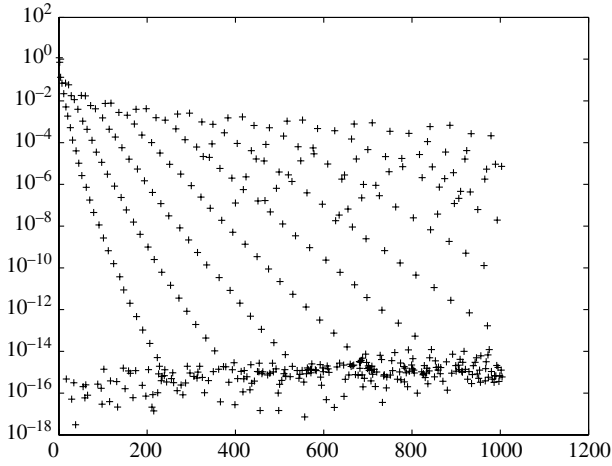


Fig. 3. Fourier coefficients for \bar{u} defined by (45) with $q = 1$

Table 2. The Galerkin method applied to Eq. (38) on the unit disk

N_λ	N_ϕ	\tilde{E}_{2w}	\tilde{E}_{G2w}	Ratio	Iterations
2	3	1.07E-1	3.29 E-1	—	4
4	6	2.89E-2	2.07 E-1	3.70	2
8	14	2.92E-2	1.14 E-1	0.98	2
16	29	1.25E-2	5.93 E-2	2.33	2
32	59	3.31E-3	3.08 E-2	3.77	2
64	121	1.13E-3	1.35 E-2	2.92	2
128	246	6.22E-4	6.74 E-3	1.81	2

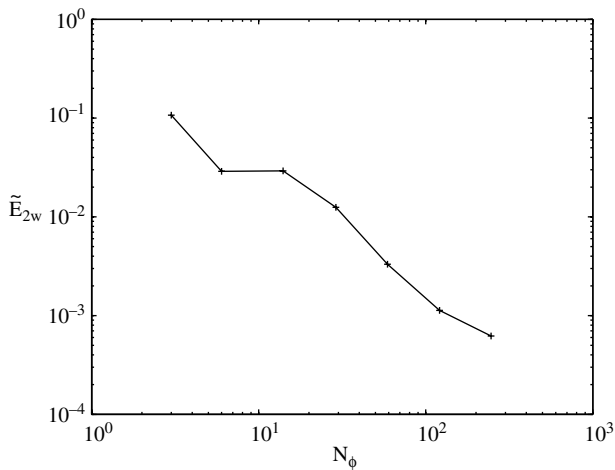


Fig. 4. Error on disk

6. Numerical Examples on the Upper Half of the Unit Disk

In the case of the upper half of the unit disk, the eigenvalues of $-\Delta$ are

$$\lambda_{m,n} = j_{m,n}^2, m = 0, 1, 2, \dots, n = 1, 2, \dots \tag{46}$$

and a set of corresponding eigenfunctions is composed by

$$u_{m,n}(x, y) = J_m(j_{m,n}r) \sin(m\theta), m = 0, 1, 2, \dots, : n = 1, 2, \dots, \tag{47}$$

where $x + iy = re^{i\theta}$. In this case

$$(u_{m,n}, u_{k,l}) = \frac{\pi}{4} [J'_m(j_{m,n})] \delta_{m,k} \delta_{n,l}. \tag{48}$$

Again the vectors $\{u_{m,n}\}_{n=1}^\infty$ form an orthogonal basis of $L^2(D)$. Here we used the procedure previously introduced for the disk, to compute the zeros of the Bessel functions and evaluate their derivatives. Notice that here the number of eigenvalues and eigenfunctions is the same, making the implementation a little easier.

For the upper half of the unit disk, we are missing the typical periodicity arguments that are important for building cubature rules on the unit disk. Consequently we use the tensorial Gauss-Legendre rule to compute an approximation of the integral in the right-hand side of (34). More precisely

$$\int_D f(x, y) dx dy \approx \sum_{j=1}^N w_j^{[0,1]} r_j \sum_{k=1}^N w_k^{[0,\pi]} f(r_j e^{i\theta_k}) r_j, \tag{49}$$

where $w_j^{[0,1]}$, r_j , $w_k^{[0,\pi]}$, θ_k are, respectively, weights and nodes in the intervals $[0, 1]$ and $[0, \pi]$. Here, we again consider (45) as our numerical example. We also give results for $q = 1$; and the number of eigenvalues is 2, 4, 8, 16, 32, 64, 128.

As a particular example here, we consider the semi-linear elliptic Eq. (38) where $g = -\Delta \bar{u} - e^{-\bar{u}}$. We choose

$$\bar{u}(x, y) = y(1 - x^2 - y^2)^q e^{x \cos(y)} \tag{50}$$

for this semi-disk case.

In this case, we have fixed in the upper half of the disk $B(0, 1)$ the points

$$(x_j, y_k) = \left(\frac{j}{10} \cos\left(\frac{k\pi}{10}\right), \frac{j}{10} \sin\left(\frac{k\pi}{10}\right) \right) \quad j, k = 0, \dots, 10$$

and then computed as in the case of the square the quantities $\tilde{E}_{2w}^{(N_\phi)}$, $\tilde{E}_{G2w}^{(N_\phi)}$ and *Ratio*: Figure 5 contains the graph of N_ϕ vs. \tilde{E}_{2w} , and it indicates that the error behavior is tending towards a linear dependence of \tilde{E}_{2w} on N_ϕ^{-1} .

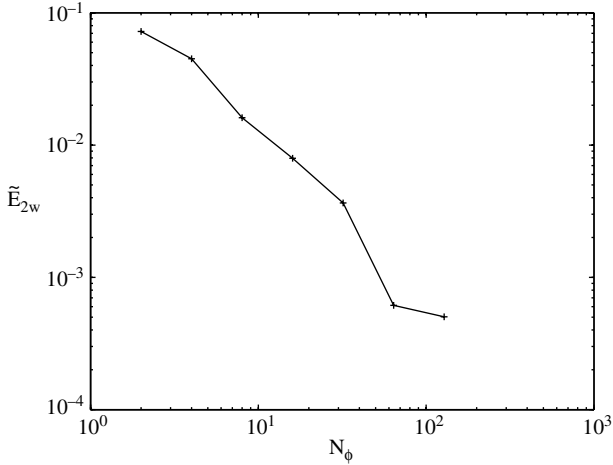


Fig. 5. Error on semidisk

Table 3. The Galerkin method applied to Eq. (38) on the semi-disk

$N_{\tilde{z}}$	N_ϕ	\tilde{E}_{2w}	\tilde{E}_{G2w}	Ratio	Iterations
2	2	7.23E-2	3.20E-1	–	3
4	4	4.49E-2	2.12E-1	1.61	3
8	8	1.61E-2	8.95E-2	2.79	2
16	16	7.95E-3	4.88E-2	2.02	2
32	32	3.65E-3	3.04E-2	2.17	2
64	64	6.14E-4	1.22E-2	5.95	2
128	128	5.03E-4	6.12E-3	1.22	2

7. Conclusions

This numerical method for solving the nonlinear problem (1) developed from the desire to avoid the numerical approximation of the singular integrals

$$\int_D G(x, y; \xi, \eta) \phi_i(\xi, \eta) d\xi d\eta \tag{51}$$

for basis functions $\{\phi_i\}$. The resulting method converges slowly, as is evidenced in both the theoretical bound (27) and the numerical examples. But in return, the approximating nonlinear algebraic system (9) is fast to set up and to solve. Our method gives reasonable approximations for not too large values of N_ϕ ; however, it would be unsuitable for very small error tolerances. We are now exploring some related methods that also avoid the need to approximate (51) but for which u_n converges more rapidly to u^* .

Acknowledgements

The work of the second author was supported by the research project CPDA028291 ‘‘Efficient approximation methods for nonlocal discrete transform’’ of the University of Padua.

References

- [1] Abramowitz, M., Stegun, I. (eds): Handbook of mathematical functions. New York: Dover Publications 1972.
- [2] Arthurs, A., Clegg, J., Nagar, A.: On the solution of the Liouville equation over a rectangle. *J. Appl. Math. Stochastic Anal.* *9*, 57–67 (1996).
- [3] Atkinson, K.: A survey of numerical methods for solving nonlinear integral equations. *J. Integral Equations Appl.* *4*, 15–46 (1992).
- [4] Atkinson, K.: The numerical solution of integral equations of the second kind. Cambridge: Cambridge University Press 1997.
- [5] Atkinson, K., Han, W.: Theoretical numerical analysis. New York: Springer 2001.
- [6] Atkinson, K., Han, W.: On the numerical solution of some semilinear elliptic problems. *Electr. Trans. Numer. Anal.* (forthcoming).
- [7] Atkinson, K., Potra, F. A.: Projection and iterated projection methods for nonlinear integral equations. *SIAM J. Numer. Anal.* *24*, 1352–1373 (1987).
- [8] Brézis, H.: Équations et inéquations non linéaires dans les espaces vectoriels en dualité. *Ann. Inst. Fourier* *18*, 115–175 (1968).
- [9] Frankel, J.: A note on the integral formulation of Kumar and Sloan. *J. Comp. Appl. Math.* *61*, 263–274 (1995).
- [10] Kelley, C.: Iterative methods for linear and nonlinear equations. *Frontiers Appl. Math.* *16*. Society for Industrial and Applied Mathematics (SIAM), Philadelphia, PA 1995.
- [11] Kelley, C., Sachs, E.: Broyden's method for approximate solution of nonlinear integral equations. *J. Integral Equations* *9*, 25–43 (1985).
- [12] Krasnoselskii, M.: Topological methods in the theory of nonlinear integral equations. London New York: Pergamon Press 1964.
- [13] Kumar, S., Sloan I.: A new collocation-type method for Hammerstein integral equations. *Math. Comp.* *48*, 585–593 (1987).
- [14] Kuttler, J. R., Sigillito, V. G.: Eigenvalues of the Laplacian in two dimensions. *SIAM Rev.* *26*, 163–193 (1984).
- [15] Stroud, A.: Approximate calculation of multiple integrals. Englewood Cliffs, N. J.: Prentice-Hall 1971.
- [16] Zeidler, E.: Nonlinear functional analysis and its applications, II/B: nonlinear monotone operators. New York: Springer 1990.

K. Atkinson
 Departments of Mathematics and
 Computer Science
 The University of Iowa
 Iowa City, IA 52242
 USA

A. Sommariva
 Department of Pure and Applied Mathematics
 University of Padua
 Padua, Italy